Nuclear Engineering and Technology 55 (2023) 1783–1790

Contents lists available at ScienceDirect

Nuclear Engineering and Technology

journal homepage: www.elsevier.com/locate/net

Original Article

Synthesis, physical, optical and radiation shielding properties of Barium-Bismuth Oxide Borate-A novel nanomaterial

B.M. Chandrika [a, b], Holaly Chandrashekara Shastry Manjunatha [a, *], K.N. Sridhar [c], M.R. Ambika [d, ***], L. Seenappa [a, **], S. Manjunatha [e], R. Munirathnam [a], A.J. Clement Lourduraj [b]

[a] Department of Physics, Government College for Women, Kolar, 563 101, Karnataka, India
[b] Department of Physics, St.Joseph's College (Autonomous), Affiliated to Bharathidasan University, Tiruchirappalli, 620 002, TamilNadu, India
[c] Department of Physics, Government First Grade College, Kolar, 563 101, Karnataka, India
[d] Department of Physics, M.S. Ramaiah Institute of Technology, Bangalore, 560 054, India
[e] Department of Chemistry, BMS College of Engineering, Bangalore, 560019, India

ARTICLE INFO

Article history:
Received 19 October 2022
Received in revised form
21 December 2022
Accepted 15 January 2023
Available online 14 February 2023

Keywords:
BBOB nanoparticles
Energy gap
Attenuation coefficient
Radiation shield
Bremsstrauhlung

ABSTRACT

Barium Bismuth Oxide Borate (BBOB) has been synthesized for the first time using solution combustion technique. SEM analysis reveal flower shape of the nanoparticles. The formation of the nanoparticles has been confirmed through XRD & FTIR studies which gives the physical and chemical structure of the novel material. The UV light absorption is observed in the range 200–300 nm. The present study highlights the radiation shielding ability of BBOB for different radiations like X/Gamma rays, Bremsstrauhlung and neutrons. The gamma shielding efficiency is comparable to that of lead in lower energy range and lesser than lead in the higher energy range. The bremsstrauhlung exposure constant is comparably larger for BBOB NPs than that of concrete and steel however it is lesser than that of lead. The beauty of BBOB nanoparticles lies in, high absorption of radiations and low emission of secondary radiations when compared to lead. In addition, the neutron shielding parameters like scattering length, absorption and scattering cross sections of BBOB are found to be much better than lead, steel and concrete. Thus, BBOB nanoparticles are highly efficient in absorbing X/Gamma rays, neutrons and bremsstrauhlung radiations.

1. Introduction

The use of radiation technology in everyday life is increasing exponentially. A few to mention imaging, radiotherapy and radio pharmaceuticals in medical, nuclear power generation, food irradiation, agriculture, industries etc. and the major concern is contamination/leakage of radiations to the environment which results in several radiation hazards. Different nuclear radiations are being used in several fields wherein shielding plays an important role in minimizing the radiation exposure and is one of the basic principles of radiation protection [1]. Design of an appropriate shielding material is a challenging task with respect to efficiency, light weight, low cost, good thermal and mechanical strength. Use of nanomaterials have become an attractive tool due to their potential properties like high surface area to volume ratio which will enable more particles to accommodate and also becomes more reactive when radiation interacts with matter. Strive for a novel material that can replace the conventional materials is still foregoing. Researchers are fascinated by using different combination of materials like metal matrix composites, glass systems, polymer composites and many more to explore the efficiency of the material.

The authors have attempted to explore different fillers used in attenuating X/Gamma rays, neutron and bremsstrahlung radiation. Lead bismuth tungstate composite was prepared by Bayoumi et al. [2] and the authors have reported that the ternary composite (Pb0.82Bi0.12WO4/W0.5Pb0.5Bi12O20) proved to be the most efficient radiation shield. Bismuth borate nanoparticles were prepared by Zhou et al. [3] by sol gel technique and have reported the high efficiency of the nanoparticle in absorbing gamma rays and

* Corresponding author.
** Corresponding author.
*** Corresponding author.
E-mail addresses: manjunathhc@rediffmail.com (H.C.S. Manjunatha), mr.ambika01@gmail.com (M.R. Ambika), seenappakolar@gmail.com (L. Seenappa).

https://doi.org/10.1016/j.net.2023.01.012

neutrons simultaneously. Lead compounds like lead sulfate, lead chloride, lead bromide, lead iodide and bismuth compounds like bismuth chloride oxide, bismuth bromide, bismuth fluoride, bismuth iodide were considered by Sayyed et al. [4] and their radiation shielding efficiency was studied. Sallam et al. [5] have investigated the physical properties and radiation shielding parameters of bismuth borate glasses doped with 0.7 wt (%) of transition metals like Cu, Co and Ni. Polydimethylsiloxane reinforced with bismuth oxide radiation shields were fabricated by Yilmaz et al. [6] and their thermal, mechanical and rheological properties were investigated. Ambika et al. [7] have studied the role of bismuth oxide in enhancing the gamma shielding ability of unsaturated polyester based polymer composites. The photon shielding performance of bismuth oxychloride doped polyester composites was investigated by Sharma et al. [8]. Many others have used bismuth and bismuth compounds as reinforcers and evaluated the gamma shielding efficiency of the compounds/composites [9,10].

The physical, optical and radiation shielding ability of PVA films containing barium titanate were studied by Issa et al. [11]. Barium iron nickel oxide nanocomposite was synthesized by solution combustion method by Sathish et al. [12] for radiation shielding applications. The structural, optical and radiation shielding ability of $BaZrO_3$ perovskite doped sodium borate glasses have been reported by Abdel et al. [13]. Seenappa et al. [14] have attempted to investigate the radiation shielding properties of barium compounds Ba_3N_2, BaF_2, BaI_2, BaS, BaSe and BaH_2. The shielding rate of barium sulphate was investigated using Monte Carlo simulations and was compared to Lead by Kim et al. [15]. Barium ferrite nanoparticles were synthesized by Reddy et al. [16], for radiation shielding and display applications.

Concrete with ferroboron and boron carbide were investigated for their neutron shielding ability by Sariyer et al. [17]. Subramanian et al. [18] have discussed the importance of boron and boron compounds for nuclear applications. Rashad et al. [19] have fabricated MgO and ZnO nanoparticles for shielding of gamma rays and fast neutrons. Sikkora et al. [20]. have made attempts to understand the effect os bismuth oxide on structural, optical and gamma/neutron shielding ability of portland cement pastes. Neutron and gamma shielding parameters were estimated for Al2O3/PbO2 nanoparticles by Ali et al. [21] Ozdemir et al. [22] have attempted to study the effect of boron trioxide on mechanical, thermal and neutron shielding ability of the EPDM composites. Gungor et al. [23] have proposed a thermal neutron shielding material consisting of EPDM and hexagonal Boron Nitride. Boron doped PVA polymeric nanofibers were prepared by Ozcan et al. [24] for absorption of neutrons in compact nuclear fusion reactors. The neutron shielding efficiency was found to be high in polyethylene/hexagonal boron nitride multilayered polymer composites by Shang et al. [25]. Seenappa et al. [26] have studied the neutron shielding parameters in some alloys such as AL-6XN, nicrosil, nisil, terfenol-D, elektron and ferro-boron.

Several researchers have reported the potential properties of bismuth, barium, boron and their compounds in absorbing X/Gamma rays and neutrons respectively [7,18]. If we have a mixture of all the three, then the material will excel in its performance. Accordingly, the authors have chosen bismuth, barium and boron compounds in the present study and synthesized Barium–Bismuth Oxide-Borate nanocomposite for the first time using green synthesis approach. The authors have made an attempt to study the structure, morphology, optical and radiation protective qualities of the novel material in detail.

2. Materials and methods

All the materials/chemicals used in the present study are of analar grade. Stoichiometric amounts of Bismuth nitrate, Barium Nitrate and Boron Nitride were taken and mixed with 25 ml of freshly extracted Aloevera gel. The mixture was kept for stirring using magnetic stirrer for homogeneous mixing and then placed in

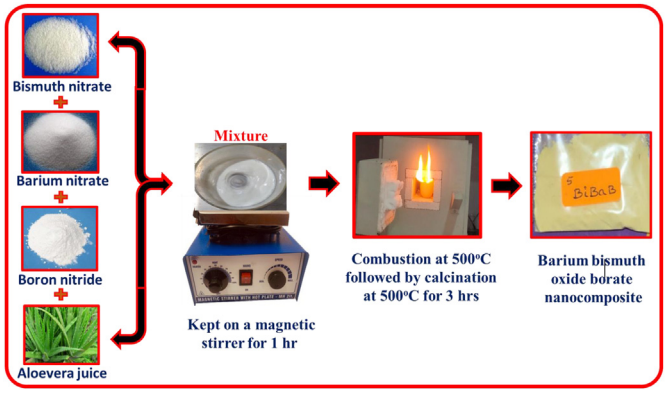

Fig. 1. Flow chart for the synthesis of Barium–Bismuth Oxide-Borate (BBOB) nanoparticles (NPs).

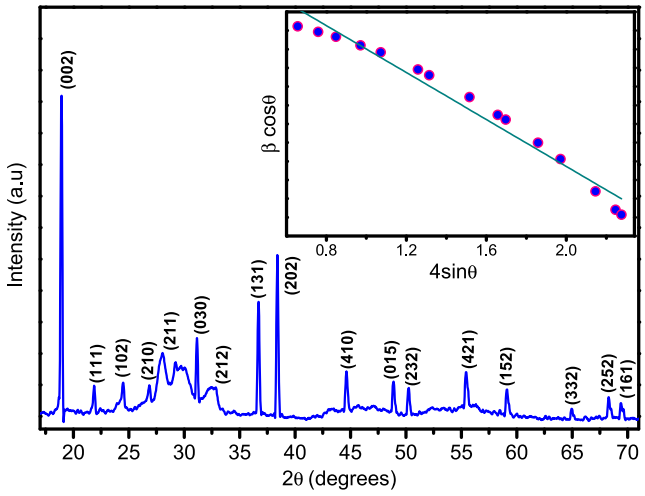

Fig. 2. PXRD pattern of BBOB NP's and (Inset: W-h plot).

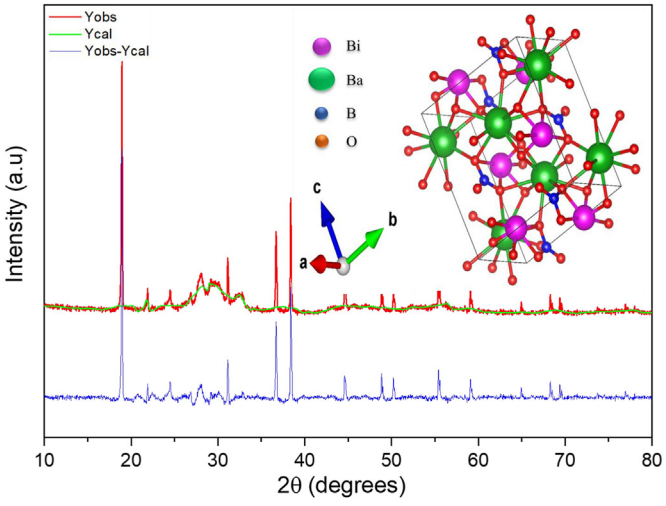

Fig. 3. Rietveld refinement (Inset: Packing diagram) of BBOB NPs.

Table 1
Crystalite size, crystallinity, strain, dislocation density and structrual factor.

Crysallite size (nm)		Crystallanity (%)	Strain× 10^{-3}	Dislocation density× 10^{15} (linm^{-2})	SF
Scherrer's	W-h				
25.51	21.84	78.42	0.63	2.09	0.4231

a muffle furnace for combustion to happen at 500^0C. Further, the obtained sample was grinded and calcination was achieved by placing the sample again in a muffle furnace at 500^0C for 3hrs. Thus, using green synthesis approach, a novel material, Barium–Bismuth Oxide-Borate (BBOB) was synthesized as shown in Fig. 1 and further characterised for their structural, optical and radiation shielding properties.

3. Results and discussion

The synthesized BBOB NP's were confirmed through the various characterization techniques such as PXRD, SEM, UV-Vis and FTIR spectroscopy.

3.1. PXRD analysis of BBOB NP's

X ray diffraction studies were conducted to study the physical structure of the nanomaterial. Several diffraction peaks are observed in Fig. 2 at 18.5, 22, 24.5, 27,28, 31, 32.5, 37, 38.5, 44.5, 49, 51, 55.5, 59, 65, 68 and 69.5 degrees, indicating the crystalline nature of the novel material. All the peaks are found to be in agreement with JCPD File No.98-042-4596. Rietveld refinement revealed

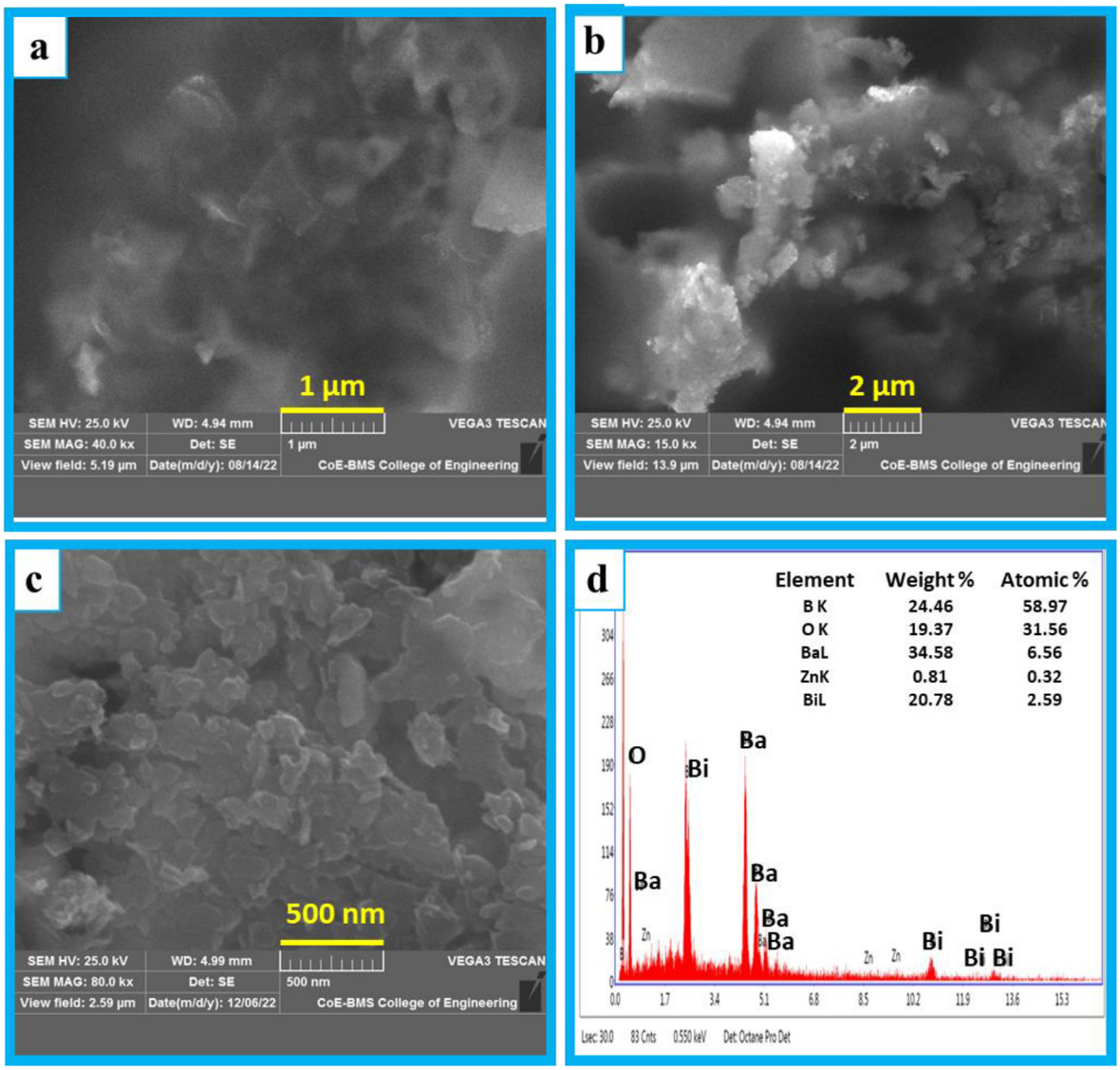

Fig. 4. (a–c) SEM image and (d) EDAX image of as-formed BBOB NPs.

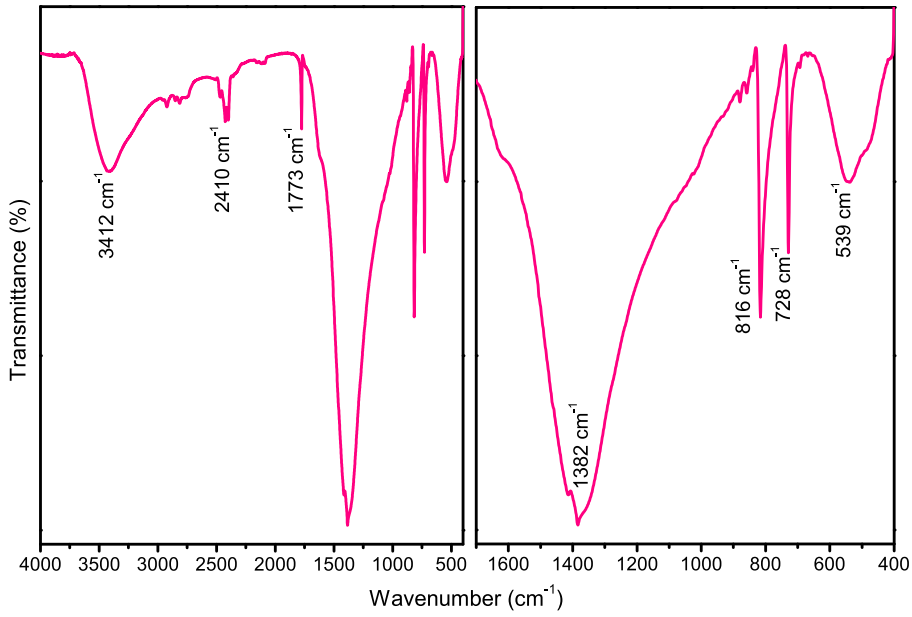

Fig. 5. FTIR spectrum of BBOB Nano particles (NPs).

Table 2
FTIR analysis.

Sl. no	Wavenumber (cm^{-1})	Remarks	Reference
1	3412	stretch vibration frequency of O-H	[27].
2	2410	C-N stretching vibrations	[28].
3	1773, 1382	BO_3 antisymmetric stretching vibrations	[29].
4	816, 728	$[BO_3]^{3-}$ group stretching vibration	[30].
5	539	$[BO_3]^{3-}$ group bending vibration	[30].

the single crystal structure of the Barium–Bismuth Oxide-Borate Fig. 3. Crystallite size and strain were calculated using Scherrer's formula and W-H Plot. The crystallite size was found to be 25.51 nm and 21.84 nm respectively. This difference in the value may be

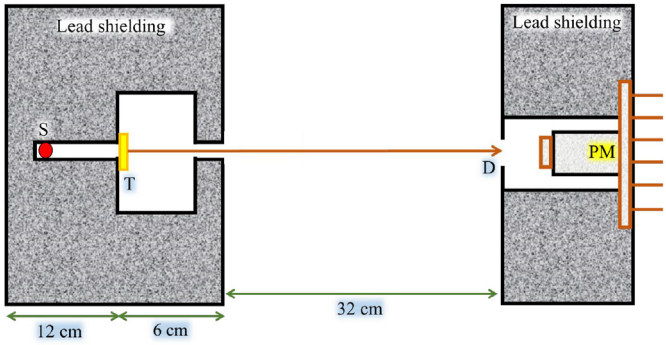

Fig. 7. Schematic diagram of the Experimental Setup (S: Source position, T: Target sample, D: Detector, PM: Photomultiplier).

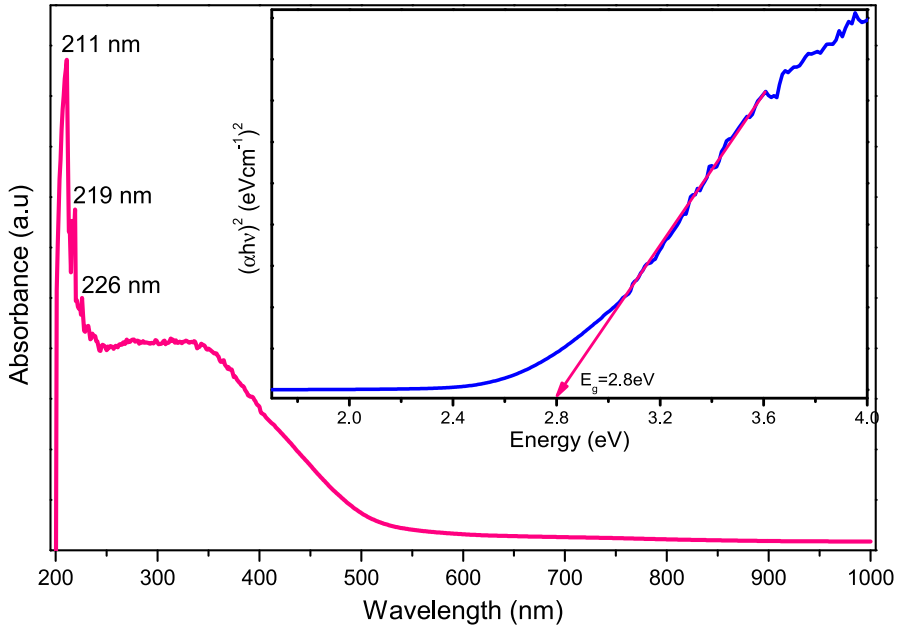

Fig. 6. UV-Visible spectrum of BBOB Nano particles (NPs).

Table 3
Comparison of measured shielding parameters for BBOB with that of theory.

E (MeV)		μ_{en}/ρ (cm^2/g)	TVL(cm)	Z_{eff}
0.276	Ex	0.29±0.02	1.86	29.49
	Th	0.22	2.39	22.83
0.365	Ex	0.20±0.007	2.77	25.40
	Th	0.12	3.65	18.09
0.511	Ex	0.13±0.01	5.37	14.82
	Th	0.12	5.36	14.81
0.662	Ex	0.13±0.005	6.66	13.67
	Th	0.12	6.64	13.66
1.173	Ex	0.04±0.001	9.72	12.46
	Th	0.04	9.71	12.45
1.332	Ex	0.04±0.001	10.55	12.32
	Th	0.04	10.54	12.31

attributed to the strain effects being considered in W-H plot. The values of various other parameters like crystallinity, strain, dislocation density and structural factor are tabulated in Table 1.

3.2. SEM analysis of BBOB NP's

SEM is a valuable tool which helps us to explore the size, distribution and shape of the nanoparticles. The morphology and elemental composition of BBOB nanoparticles have been presented in Fig. 4. It is evident from the figure that, the particles appear to be like a flower. On the other hand, slight agglomeration has been noticed in Fig. 4b. The formation of nanoflower shape particle has been confirmed in the present study of 500 nm resolution (Fig. 4b). In addition, the elemental composition of boron, oxygen, barium and bismuth are 24.46, 19.37, 35.39 and 20.78 wt (%) respectively.

3.3. FTIR analysis of BBOB NP's

FTIR studies reveal the chemical structure of BBOB nanoparticles. The FTIR spectra of BBOB nanoparticles is shown in Fig. 5 in the range 400–4000 cm^{-1}. The presence of absorption peaks is evident from the figure and the so called finger print region in the range 400 cm^{-1} and 1500 cm^{-1}. The stretching, bending vibrations assigned to the different functional group have been presented in Table 2. The presence of C-N groups is due to the fact that the green extract is used as the reducing agent in the synthesis. The formation of BBOB nanoparticles is confirmed through the presence of all these functional groups.

3.4. UV-Visible spectroscopic analysis of BBOB NP's

The optical absorption spectra of BBOB nanoparticles is shown in Fig. 6 and the inset graph is the Tauc's plot. It is evident from the figure that, the absorption of photon increases with increase in the wavelength and peaks at three wavelengths 211, 219 and 226 nm showing UV light absorption in 200–300 nm range. The energy needed to excite an electron from valence band to conduction band is found to be 2.8eV (Eg) from the Tauc's plot. This may be attributed to the presence of bismuth, barium and boron in the mixture [31–33]. The band gap of any semiconductor can be tuned by varying the size of the particle. Smaller the size of the particle, greater is the band gap due to quantum size effects and hence smaller the wavelength of light emitted [34].

3.5. Gamma shielding characteristics

We have measured the X-ray/gamma absorption properties in BBOB nano particles. NaI(Tl) detector coupled with MCA is used in

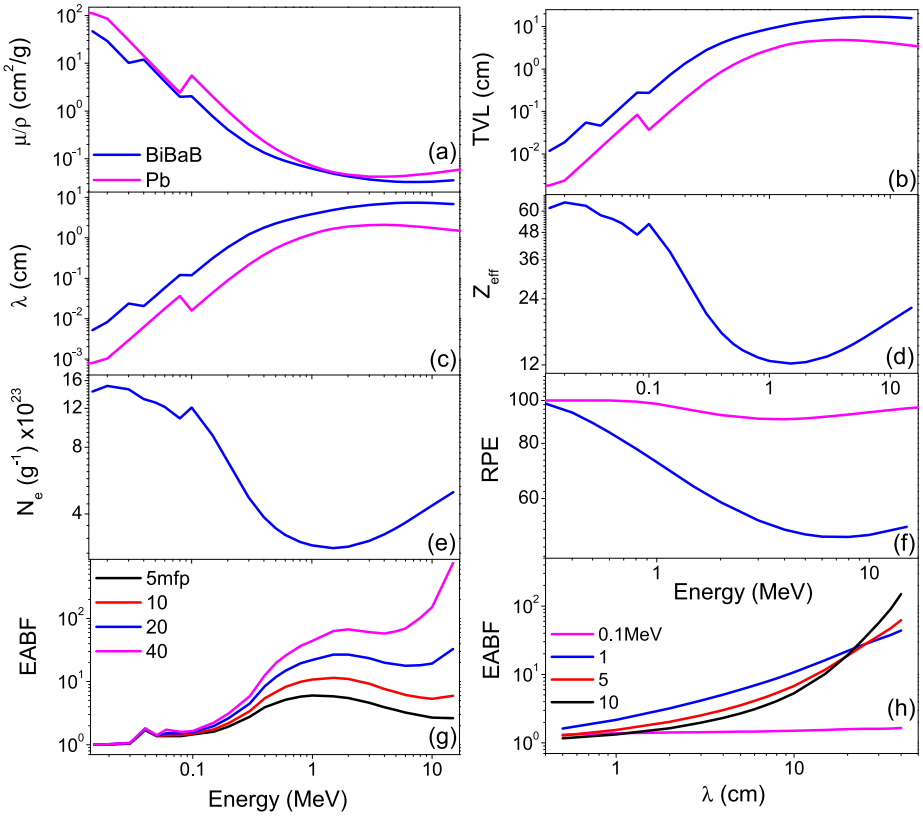

Fig. 8. X-ray/gamma shielding parameters: (a) Mass attenuation coefficient vs energy (b) TVL vs energy c) Mean free path vs energy, (d) Effective atomic number vs energy,(e) Effective electron density vs energy, (f) Radiation protection efficiency of BBOB NPs with that of lead,(g) EABF vs energy, (h) EABF vs mean free path for BBOB NPs.

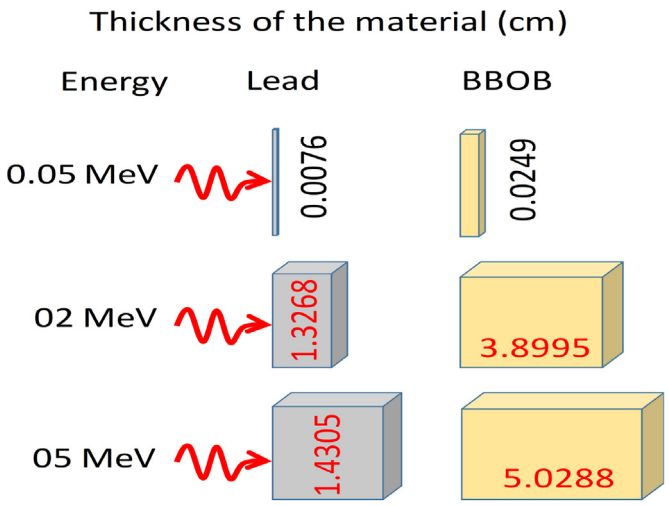

Fig. 9. Comparison of thickness of materials required to stop 0.05 MeV, 2 MeV and 5 MeV.

the measurement. Further details of the experiment is explained in the previous reports [12,35–37]. The experimental setup used for the measurement of X-ray/gamma ray shielding properties of BBOB nano particles is provided in Fig. 7.

The mass attenuation coefficient of the sample is calculated from the measured integral intensities. The derivable of the measured mass attenuation coefficient such as TVL and effective atomic number is computed from measured mass attenuation coefficient. The comparison of the measured values with that of the theory is as shown in the Table 3.

After the validation of present work, we have studied other shielding parameters. The mass attenuation coefficient of BBOB nanoparticle is found to decrease with increase in energy and peaks at 0.09 MeV and further decreases with increase in energy due to decrease in interaction cross section as evident from Fig. 8a. During the interaction, gamma photons transfer their energy through several processes like photoelectric effect, compton effect and pair production process, which are infact energy dependent. The tenth value layer thickness is the essential parameter for any practical applications. The relaxation length and TVL values increases with increase in gamma photon energy and are presented in Fig. 8b and c. Lower the relaxation length, higher will be the shielding efficiency of the said material. The attenuation of gamma photons depends on the atomic number of the absorber. Since, the material is a compound which consists of bismuth, barium, boron and oxygen, the Z of the material cannot be defined, hence we define effective atomic number (Z_{eff}) which decreases with increase in photon energy as shown in Fig.(8)d. Similar trend of variation is observed for electron density Fig. 8e. The radiation protection efficiency is maximum in the lower energy range and decreases gradually with increase in energy Fig. 8f. The EABF values are found to vary with respect to gamma photon energy and mean free path as evident from Fig. 8g and h. EABF is observed to be minimum in the lower energy range and further increases with increase in energy. All these variations may be attributed to the dominance of photoelectric effect, compton effect and pair production processes in the lower, medium and higher energy range respectively [38,39]. The gamma shielding ability of the nanoparticle is compared to that of lead which is the conventional shielding material. The attenuation coefficient and TVL values are comparable (lesser) to that of lead. Hence, the BBOB nanoparticles can be used for low energy gamma shielding applications.

For an instance, we have shown in Fig. 9, the thickness of the synthesized novel material BBOB and lead required to reduce the intensity of gamma photons to half of its actual intensity. The standard and conventional shielding material lead requires 0.0076, 1.3268, 1.4305 cm to stop gamma rays of energy 0.05, 2, 5 MeV respectively, whereas BBOB requires 0.0249, 3.8995 and 5.0288 cm. Thus, the HVL values of the novel material is comparable to lead in lower energy and greater than lead in higher energy range. Thus, the material serves as a good candidate for shielding of low energy gamma rays.

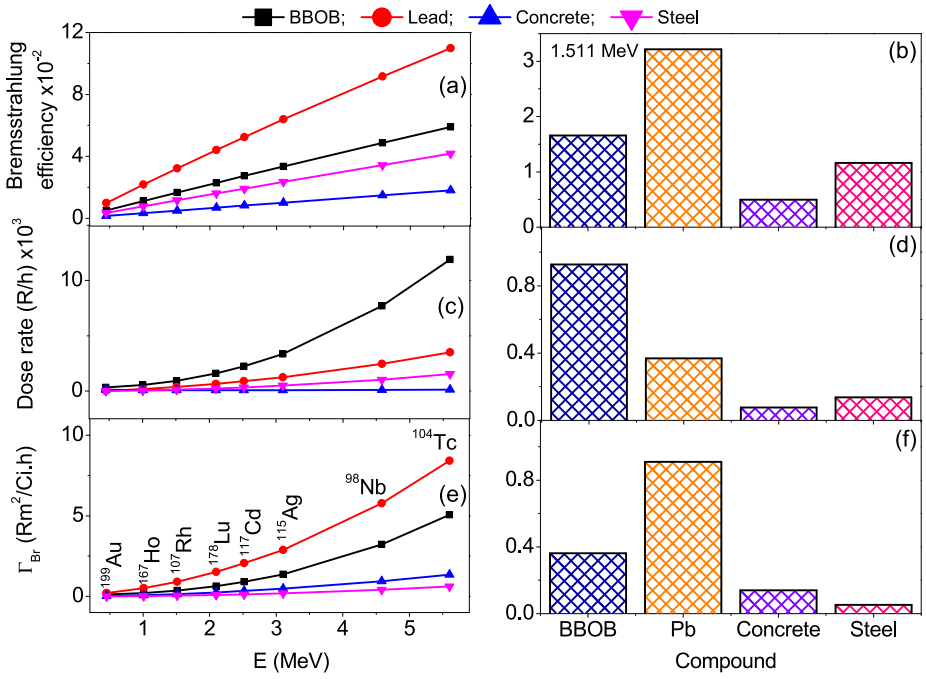

Fig. 10. Bremsstrahlung shielding parameters for Lead, concrete and steel at different energies: (a) Variation of bremsstrahlung efficiency/yield vs energy, (b) Comparison of bremsstrahlung efficiency among lead, concrete and steel at 1.511 MeV, (c) Variation of bremsstrahlung dose rate vs energy, (d) Comparison of bremsstrahlung dose rate among lead, concrete and steel at 1.511 MeV, (e) Variation of specific bremsstrahlung constant vs energy & (f) Comparison of specific bremsstrahlung constant among lead, concrete and steel at 1.511 MeV.

3.6. Bremsstrahlung characteristics

Usually high Z compounds/mixtures are preferred for the shielding of X-ray/gamma radiations, because the absorption of X-ray/gamma radiation is directly proportional to the atomic number of the target medium. However, the disadvantage of using high Z compounds/mixtures in the X-ray/gamma radiation shielding is the production of secondary radiations such as bremsstrahlung. Radiation shielding is required for the place where the nuclear reactions are carried out. During the nuclear reactions, along with the X-ray/gamma radiations, alpha and beta radiations are also emitted. There is no issue with the emitted alpha particle which is simply absorbed in the high Z compounds/mixtures. Whereas the beta which were emitted during the nuclear reactions interacts with the high Z atoms in the targets and produces the bremsstrahlung radiation which comes in the X-ray region. The production of bremsstrahlung is also directly proportional to the atomic number of the target. Eventually, to absorb X-ray/gamma radiations effectively, secondary radiations such as bremsstrahlung are produced. Thus, to design the shielding for X-ray/gamma radiations, we must consider the secondary radiations such as bremsstrahlung also. A good shielding material for X-ray/gamma should not produce large amount of secondary radiations also. Thus, in the present study, bremsstrahlung shielding parameters such as bremsstrahlung dose rate, bremsstrahlung efficiency and specific bremsstrahlung constant are also evaluated using the theoretical formalism explained in the previous work [40–42] with the help of measured EDAX composition. The evaluated bremsstrahlung shielding parameters is shown in the Fig. 10.

Bremsstrahlung efficiency signifies the quantity of secondary radiation produced by the beta during interaction with the target medium. Fig. 10a shows the variation of bremsstrahlung efficiency as a function of energy of interacting beta particle for the synthesized BBOB along with the traditional shielding materials such as lead, concrete and steel. From this comparison (Fig. 10d) it is found that bremsstrahlung production is large for lead when it compares with the other materials studied. Meanwhile, bremsstrahlung effficiency of BBOB NPs are less than that of lead. The energy of the bremsstrahlung radiations absorbed in the medium is given by bremsstrahlung dose rate. The variation of bremsstrahlung dose rate as a function of energy of the interacting beta is also given in Fig. 10b. The comparison of bremsstrahalung dose rate among the studied materials (.10e) reveals that bremsstrahlung dose rate is larger for BBOB NPs than that of the other studied materials. It is also found that from the Fig. 10c, specific bremsstrahlung exposure constant is comparably larger for BBOB NPs than that of concrete and steel however it is lesser than that of lead. By studying the bremsstrahlung shielding parameter it is observed that the synthesized NPs produces smaller quantity of secondary radiation such as bremsstrahlung when it is compared to lead meanwhile, bremsstrahlung absorption is also large in the synthesized NPs. The good shielding material should have the property of not producing secondary radiation (Bremsstrahlung) including good absorbing of primary radiations. In view of this, the lower emission of bremsstrahlung radiation also considered as the good characteristic of shielding material.

3.7. Neutron shielding characteristics

Neutrons interact with the material medium through absorption and scattering processes. Hence, estimation of neutron shielding parameters like neutron absorption cross section, scattering cross section, scattering length and attenuation parameter are equally important, since, the nanomaterial consists of both high Z and low Z material. All these parameters are estimated using the data for elements adopted from previous work [43] and measured elemental composition EDAX by following mixture rule. The evaluated neutron shielding parameters for BBOB NPs are compared with that of conventional shielding materials like lead, concrete and steel. The relaxation length is found to be 4 fm which is less than that of lead, concrete and steel from Fig. 11a. The scattering cross section, absorption cross section and scattering length is high compared to the conventional materials as evident from Fig. 11b,c,d. Hence, proves to be the best than any traditional shielding materials.

4. Summary

In the present study, solution combustion technique was used to synthesize a novel nanomaterial Barium–Bismuth Oxide-Borate for the first time. The nanoflower shape of the nanoparticle has been

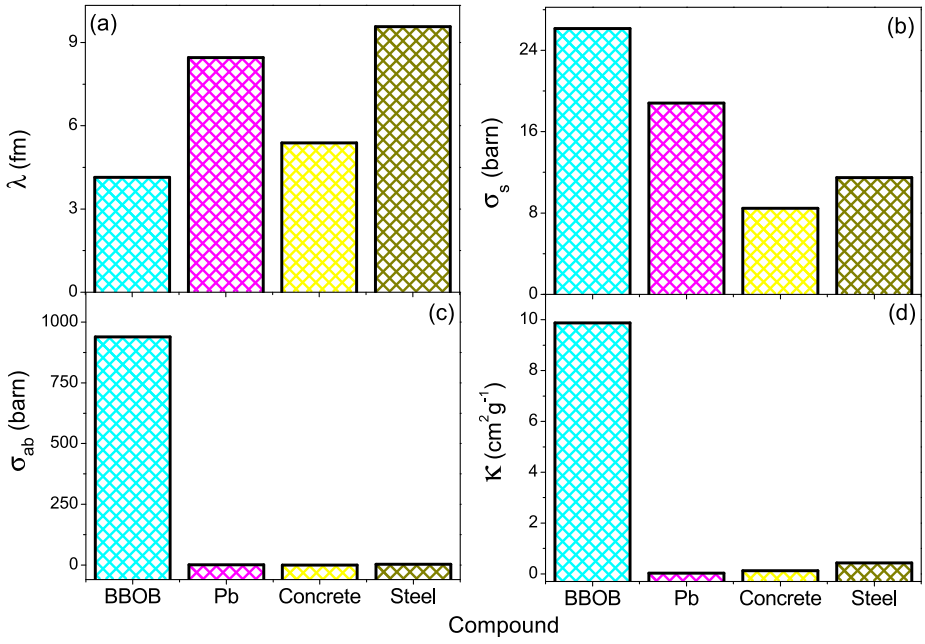

Fig. 11. Comaparison of neutron shielding parameters:(a) Neutron scattering length (λ (fm)) (b) Neutron scattering cross section (σ_s (barn)) (c) Neutron absorption cross section (σ_{ab} (barn)) (d) Neutron attenuation parameter ($\kappa(cm^2g^{-1})$).

explored through SEM images. The formation of BBOB nanoparticles has been confirmed through FTIR studies. X ray diffraction technique reveal the crystal structure of the said material. The radiation protective qualities of the novel nanomaterial has been discussed in detail and the results reveal that, BBOB nanoparticles are highly efficient in absorbing low energy gamma photons and also possess excellent neutron shielding ability compared to lead. Moreover, emission of bremsstralung radiation is less compared to lead. Thus, conventional material like lead, concrete and steel can be replaced by BBOB nanomaterial as they are good absorbers of X/Gamma rays, neutrons and bremsstrahlung radiations.

Declaration of competing interest

The authors declare that they have no known competing financial interests or personal relationships that could have appeared to influence the work reported in this paper.

All the authors have contributed and given their consent towards the submission.

References

[1] J.E. Martin, Physics for Radiation Protection: a Handbook, John Wiley & Sons, 2006.

[2] E.E. Bayoumi, M.O. Abd El-Magied, E.A. Elshehy, B.M. Atia, K.A. Mahmoud, L.H. Khalil, A.A. Mohamed, Lead−bismuth tungstate composite as a protective barrier against gamma rays, Mater. Chem. Phys. 275 (2022), 125262.

[3] D. Zhou, Q.-P. Zhang, J. Zheng, Y. Wu, Y. Zhao, Y.-L. Zhou, Co-shielding of neutron and γ-ray with bismuth borate nanoparticles fabricated via a facile sol-gel method, Inorgan. Chem. Commun. 77 (2017) 55.

[4] M.I. Sayyed, F. Akman, M.R. Kaçal, A. Kumar, Radiation protective qualities of some selected lead and bismuth salts in the wide gamma energy region, Nuclear Eng. Technol. 51 (2019) 860.

[5] O. Sallam, A.M. Madbouly, N.A. Elalaily, F.M. Ezz-Eldin, Physical properties and radiation shielding parameters of bismuth borate glasses doped transition metals, J. Alloys Compounds 843 (2020), 156056.

[6] S.N. Yılmaz, A. Güngör, T. Özdemir, The investigations of mechanical, thermal and rheological properties of polydimethylsiloxane/bismuth (iii) oxide composite for x/gamma ray shielding, Radiat. Phy. Chem. 170 (2020), 108649.

[7] M.R. Ambika, N. Nagaiah, S.K. Suman, Role of bismuth oxide as a reinforcer on gamma shielding ability of unsaturated polyester based polymer composites, J. Appl. Poly. Sci. 134 (2017).

[8] A. Sharma, M.I. Sayyed, O. Agar, M.R. Kaçal, H. Polat, F. Akman, Photon-shielding performance of bismuth oxychloride-filled polyester concretes, Mater. Chem. Phys. 241 (2020), 122330.

[9] E.-S.A. Waly, G.S. Al-Qous, M.A. Bourham, Shielding properties of glasses with different heavy elements additives for radiation shielding in the energy range 15−300 kev, Radiat. Phys. Chem. 150 (2018) 120.

[10] M. Kamislioglu, Research on the effects of bismuth borate glass system on nuclear radiation shielding parameters, Result. Phys. 22 (2021), 103844.

[11] S.A.M. Issa, H.M.H. Zakaly, M. Pyshkina, M.Y.A. Mostafa, M. Rashad, T.S. Soliman, Structure, optical, and radiation shielding properties of pva−batio3 nanocomposite films: an experimental investigation, Radiat. Phys. Chem. 180 (2021), 109281.

[12] K.V. Sathish, H.C. Manjunatha, Y.S. Vidya, K.N. Sridhar, L. Seenappa, B.C. Reddy, S.A.C. Raj, P.S.D. Gupta, X-rays/gamma rays radiation shielding properties of barium−nickel−iron oxide nanocomposite synthesized via low temperature solution combustion method, Radiat. Phys. Chem. 194 (2022), 110053.

[13] M. Abdel Maksoud, S.M. Kassem, O. Sallam, Structural, optical, and radiation shielding features of newly developed bazro3/na2o−b2o3 glass, Ceram.Int. 48 (2022), 30938.

[14] L. Seenappa, H.C. Manjunatha, B.M. Chandrika, H. Chikka, A study of shielding properties of x-ray and gamma in barium compounds, J. Radiat. Protec. Res. 42 (2017) 26.

[15] S. Kim, K. Kim, J. Park, Barium compounds through monte carlo simulations compare the performance of medical radiation shielding analysis, J. Kor. Soc. Radiol. 7 (2013) 403.

[16] B.C. Reddy, Y.S. Vidya, H.C. Manjunatha, K.N. Sridhar, U.M. Pasha, L. Seenappa, B. Sadashivamurthy, N. Dhananjaya, B.M. Sankarshan, S. Krishnaveni, et al., Synthesis and characterization of barium ferrite nano-particles for x-ray/gamma radiation shielding and display applications, Prog. in Nuclear Energy 147 (2022), 104187.

[17] D. Sarıyer, R. Küçer, N. Küçer, Neutron shielding properties of concretes containing boron carbide and ferro−boron, Proc. Soc. Behav. Sci. 195 (2015) 1752.

[18] C. Subramanian, A.K. Suri, T.S.R.C. Murthy, Development of boron-based materials for nuclear applications, Barc. Newsl. 313 (2010) 14.

[19] M. Rashad, H. Tekin, H.M. Zakaly, M. Pyshkina, S.A. Issa, G. Susoy, Physical and nuclear shielding properties of newly synthesized magnesium oxide and zinc oxide nanoparticles, Nuclear Eng. Technol. 52 (2020) 2078.

[20] P. Sikora, A.M. El-Khayatt, H. Saudi, S.-Y. Chung, D. Stephan, M. Abd Elrahman, Evaluation of the effects of bismuth oxide (bi2o3) micro and nanoparticles on the mechanical, microstructural and γ-ray/neutron shielding properties of portland cement pastes, Construct. Build. Mater. 284 (2021), 122758.

[21] A.M. Ali, S.A. Issa, M.R. Ahmed, Y.B. Saddeek, M.H.M. Zaid, M. Sayed, H.H. Somaily, H.O. Tekin, K.A. Matori, H.M. Zakaly, et al., Promising applicable heterometallic al2o3/pbo2 nanoparticles in shielding properties, J. Mater. Res. Technol. 9 (2020), 13956.

[22] T. Özdemir, A. Güngör, İ. Reyhancan, Flexible neutron shielding composite material of epdm rubber with boron trioxide: mechanical, thermal investigations and neutron shielding tests, Radiat. Phys. Chem. 131 (2017) 7.

[23] A. Güngör, I.K. Akbay, T. Özdemir, Epdm rubber with hexagonal boron nitride: a thermal neutron shielding composite, Radiat. Phys. Chem. 165 (2019), 108391.

[24] M. Özcan, E. Kam, C. Kaya, F. Kaya, Boron-containing nonwoven polymeric nanofiber mats as neutron shields in compact nuclear fusion reactors, Int. J. Energy Res. 46 (2022) 7441.

[25] Y. Shang, G. Yang, F. Su, Y. Feng, Y. Ji, D. Liu, R. Yin, C. Liu, C. Shen, Multilayer polyethylene/hexagonal boron nitride composites showing high neutron shielding efficiency and thermal conductivity, Compos. Commun. 19 (2020) 147.

[26] L. Seenappa, H.C. Manjunatha, B.M. Chandrika, K.N. Sridhar, C. Hanumantharayappa, Study of Gamma, X-Ray and Neutron Shielding Parameters of Some Alloys, 2018.

[27] Y. Astuti, A. Fauziyah, S. Nurhayati, A.D. Wulansari, R. Andianingrum, A.R. Hakim, G. Bhaduri, Synthesis of α-bismuth oxide using solution combustion method and its photocatalytic properties, in: IOP Conference Series: Materials Science and Engineering vol. 107, IOP Publishing, 2016, 012006.

[28] A.Z. Bazeera, M.I. Amrin, Synthesis and characterization of barium oxide nanoparticles, IOSR J. Appl. Phys. 1 (2017) 76.

[29] X. Dong, S. Pan, F. Li, Y. Shi, Z. Zhou, W. Zhao, Z. Huang, Synthesis, growth, crystal structure and optical properties of babibo4, Inorgan. Chem. Commun. 23 (2012) 109.

[30] P.M. Rafailov, A.V. Egorysheva, T.I. Milenov, V.D. Volodin, G.V. Avdeev, R. Titorenkova, V.M. Skorikov, R. Petrova, M.M. Gospodinov, Synthesis, growth and optical spectroscopy studies of babibo4 and cabi2b2o7 crystals, Appl. Phys. B 101 (2010) 185.

[31] D. Pérez-Mezcua, R. Sirera, R. Jiménez, I. Bretos, C. De Dobbelaere, A. Hardy, M.K. Van Bael, M.L. Calzada, A uv-absorber bismuth (iii)-n-methyldiethanolamine complex as a low-temperature precursor for bismuth-based oxide thin films, J. Mater. Chem. C 2 (2014) 8750.

[32] B. Singh, G. Kaur, P. Singh, K. Singh, B. Kumar, A. Vij, M. Kumar, R. Bala, R. Meena, A. Singh, et al., Nanostructured boron nitride with high water dispersibility for boron neutron capture therapy, Sci. Rep. 6 (2016) 1.

[33] S. Sun, W. Xiao, C. You, W. Zhou, Z.N. Garba, L. Wang, Z. Yuan, Methods for preparing and enhancing photocatalytic activity of basic bismuth nitrate, J. Clean. Product. 294 (2021), 126350.

[34] D. Patidar, K.S. Rathore, N.S. Saxena, K. Sharma, T.P. Sharma, Energy band gap studies of cds nanomaterials, in: Journal of Nano Research vol. 3, Trans Tech Publ, 2008, pp. 97−102.

[35] K.V. Sathish, H.C. Manjunatha, Y.S. Vidya, K.N. Sridhar, L. Seenappa, B.C. Reddy, S.A.C. Raj, S. Manjunatha, P.S.D. Gupta, R. Munirathnam, Investigations on radiation shielding properties of leadaluminoborate nanocomposite, Prog. Nuclear Energy 150 (2022), 104310.

[36] B.C. Reddy, H.C. Manjunatha, Y.S. Vidya, K.N. Sridhar, U.M. Pasha, L. Seenappa, B. Sadashivamurthy, N. Dhananjaya, K.V. Sathish, P.S.D. Gupta, X-ray/gamma ray radiation shielding properties of α-bi2o3 synthesized by low temperature solution combustion method, Nuclear Eng. Technol. 54 (2022) 1062.

[37] B.C. Reddy, H.C. Manjunatha, Y.S. Vidya, K.N. Sridhar, U.M. Pasha, L. Seenappa, C. Mahendrakumar, B. Sadashivamurthy, N. Dhananjaya, B. Sankarshan, et al., Synthesis and characterization of multi functional nickel ferrite nano-particles for x-ray/gamma radiation shielding, display and antimicrobial applications, J. Phy. Chem. Solids 159 (2021), 110260.

[38] H. Manjunatha, K. Sathish, L. Seenappa, D. Gupta, S.A. Cecil Raj, A study of x-ray, gamma and neutron shielding parameters in si- alloys, Radiat. Phys. Chem. 165 (2019), 108414.

[39] K.V. Sathish, H.C. Manjunatha, Y.S. Vidya, B.M. Sankarshan, P.S.D. Gupta, L. Seenappa, K.N. Sridhar, A.C. Raj, Investigation on shielding properties of lead based alloys, Prog. Nuclear Energy 137 (2021), 103788.

[40] H.C. Manjunatha, B.M. Chandrika, Beta-induced bremsstrahlung shielding parameters in various types of steels, Radiat. Eff. Defect. Solids 174 (2019) 542.

[41] H.C. Manjunatha, A dosimetric study of beta induced bremsstrahlung in bone, Appl. Radiat. Isotopes 94 (2014) 282.

[42] H.C. Manjunatha, Dose assessment of bremsstrahlung induced by beta-emitting radioisotopes of uranium-238 series and lead in human tissues, Isotopes Environ. Health Stud. 50 (2014) 555.

[43] H.C. Manjunatha, K.N. Sridhar, Empirical formula for neutron scattering lengths and cross sections, Nuclear Instrum. Method. Phys. Res. Section A: Accelerat. Spectrom. Detect. Assoc. Equipment 877 (2018) 349.